Journal of Solid State Chemistry 182 (2009) 1377–1386

Contents lists available at ScienceDirect

Journal of Solid State Chemistry

journal homepage: www.elsevier.com/locate/jssc

Channels occupancy and distortion in new lithium uranyl phosphates with three-dimensional open-frameworks

C. Renard *, S. Obbade, F. Abraham

Unité de Catalyse et de Chimie du Solide (CNRS UMR 8181), ENSC Lille–UST Lille, BP 90108, 59652 Villeneuve d'Ascq cedex, France

ARTICLE INFO

Article history:
Received 10 December 2008
Received in revised form
13 February 2009
Accepted 16 February 2009
Available online 26 February 2009

Keywords:
Uranyl phosphate
Solid state synthesis
Crystal structure
Three-dimensional framework
Cationic conductivity

ABSTRACT

Three new lithium uranyl phosphates, $Li_2(UO_2)_3(PO_4)_2O$ (**1**), $Li(UO_2)_4(PO_4)_3$ (**2**) and $Li_3(UO_2)_7(PO_4)_5O$ (**3**) were synthesized and studied. Powders of **1** and **2** were synthesized via solid state reaction, and single crystals of the three compounds were obtained by melting of **1** and **2** powders. The structures of the three compounds have been solved and refined from single crystal X-ray diffraction data. In the three compounds, the uranium atoms occupy square and pentagonal bipyramids. The uranium square bipyramids and phosphate tetrahedra are connected by vertices to form two types of layers with autunite sheet anion-topology $^2_\infty[(UO_2)(PO_4)_2]^{4-}$ and $^2_\infty[(UO_2)_2(PO_4)_3]^{5-}$denoted S and D, respectively. The uranyl pentagonal bipyramids share opposite equatorial edges to form $^1_\infty[UO_5]^{4-}$ infinite chains. Mutually perpendicular chains are hung on each side of the sheets to build frameworks with non-crossing perpendicular channels that accommodate the lithium ions. Various stacking sequences of the S and D layers, S–S, D–D and S–D, generate three different frameworks in **1**, **2** and **3**, respectively. These compounds are similar to the recently reported vanadate analogous. However, the phosphate tetrahedra, smaller than the vanadate ones, gives distortion of the layers and a lowering of the symmetry and/or a change of periodicity. The electrical conductivity of **1** and **2** was measured using impedance spectroscopy method. The rather low conductivity of the lithium cations is explained by the crystal structure and the Li^+ position within the tunnels. These results corroborate those on the analogous three-dimensional alkaline uranyl vanadates. Crystallographic data: 293 K, BRUKER X8-APEX2 X-ray diffractometer, 4 K CCD detector, Mo$K\alpha$, $\lambda = 0.71073$ Å, full-matrix least-squares refinement on the basis of *F*. **1**, Tetragonal symmetry, space group $I4_1/amd$, $Z = 4$ with $a = 7.1109(2)$ Å and $c = 25.0407(8)$ Å, $R = 0.034$ and w$R = 0.047$ for 38 parameters with 479 independent reflections with $I \geqslant 3\sigma(\mathbf{I})$. **2**, monoclinic symmetry, space group $P2_1/c$, $Z = 4$ and $a = 9.8829(2)$ Å, $b = 9.8909(2)$ Å, $c = 17.4871(4)$ Å and $\beta = 106.198(1)^\circ$, $R = 0.021$ and w$R = 0.031$ for 249 parameters with 4201 independent reflections with $I \geqslant 3\sigma(\mathbf{I})$. **3**, Tetragonal symmetry, space group $P\bar{4}2_1m$ with $a = 9.9305(2)$ Å and $c = 14.5741(3)$ Å, $R = 0.035$ and w$R = 0.038$ for 137 parameters with 4527 independent reflections with $i \geqslant 3\sigma(\mathbf{I})$.

1. Introduction

The uranyl phosphates represent a significant part of the uranium minerals. Their crystal structures are mostly two-dimensional with low valence cations and/or water molecules in the interlayer space between uranyl phosphate layers. The autunite and phosphuranylite groups are the two main mineral families, their structures are based on sheets with U:P = 1:1 and 3:2, respectively. The autunite-type sheet with formula $^2_\infty[(UO_2)(PO_4)_2]^{4-}$ is built on corner shared uranyl square bipyramids and phosphate tetrahedra [1–3]. The phosphuranylite-type sheet with formula $^2_\infty[(UO_2)_3(O_{2-x}OH_x)(PO_4)_2]^{(4-x)-}$ $(x = 0,1,2)$ is made up of ribbons of edge shared hexagonal and pentagonal uranium bipyramids further connected by phosphate tetrahedra. In some minerals, the interlayer space is occupied by various combinations of monovalent, divalent or trivalent ions and water molecules. However, in the phosphuranylite mineral [4], uranyl ions are located in the interlayer space with the uranyl ions parallel to the sheet, the corresponding uranium being in a square bipyramidal coordination. Similarly in vanmeerscheite mineral [5] non-uranyl U^{6+} ions occupy the interlayer space and are in a distorted octahedral environment. For the two compounds, these UO_6 polyhedra link the sheets to form a pillared-layers three-dimensional open framework that releases large cavities to insert cations or small molecules. Uranophane-type layers connected by UO_7 pentagonal bipyramids form another uranyl phosphate pillared-layers structural family [6–8]. In general, the uranyl oxygen atoms are non-bridging and the $(UO_2)^{2+}$ ion presence

* Corresponding author. Fax: +33 3 20 43 68 14.
E-mail address: catherine.renard@ensc-lille.fr (C. Renard).

0022-4596/$ - see front matter © 2009 Elsevier Inc. All rights reserved.
doi:10.1016/j.jssc.2009.02.024

facilitates the sheet formation; only equatorial uranium oxygen atoms provide the connectivity with the oxoanion polyhedra. In the two above reported examples, the UO_6 and UO_7 pillars share equatorial oxygen of the uranyl ions with the phosphate tetrahedra of the uranyl phosphate layers. A U/P ratio less than 1 favors three-dimensional structures by the creation of polyphosphate units. $Na_2(UO_2)(P_2O_7)$ [9], $Cs(UO_2)(PO_3)_3$ [10] and $UO_2H(PO_3)_3$ [11] are some examples of uranyl polyphosphate three-dimensional frameworks. Recently, the two structure of two new lithium uranyl phosphates, α-Li$[(UO_2)(PO_4)]$ and $Li_2[(UO_2)_3(P_2O_7)_2]$, has been reported [12], the three-dimensional framework results from the sharing of vertices of the uranyl and phosphate polyhedra.

The uranyl vanadates crystal chemistry is rather different, in particular because the vanadium atom can adopt tetrahedral and square pyramidal environment. The uranium coordination polyhedron is mostly a pentagonal bipyramid. The uranyl ion also favors two-dimensional structures. The layered carnotite-type structure is the most common one [13–21], in this structure, dimers of edge shared UO_7 pentagonal bipyramids and dimers of edge shared VO_5 square pyramids are formed and further connected to form sheets. With tetrahedral vanadium, uranyl polyhedra can build uranophane type sheets with two-dimensional structures as in the recently diamine templated uranyl vanadates [22] or three-dimensional structures as in $(UO_2)_2V_2O_7$ [23,24] where the sheets are connected by sharing non-sheet corners of the vanadate tetrahedra to form di-vanadate entities or in $(UO_2)_3(VO_4)_2(H_2O)_5$ [25] where the sheets are pillared by UO_7 pentagonal bipyramids. Three-dimensional frameworks are also obtained from isolated UO_7 polyhedra connected to di-vanadate units by corner sharing in $Pb(UO_2)(V_2O_7)$ [26] or from $^1_\infty[UO_6]$ chains of UO_7 polyhedra connected by cation–cation interactions and $(VO_3)_n$ metavanadate-type chains of corner-sharing VO_4 tetrahedra in UV_2O_8 which can be considered as a uranyl metavanadate $(UO_2)(VO_3)_2$ [24]. Lately, Obbade et al. have described new monovalent cation uranyl vanadate families with three-dimensional structures, $A_2(UO_2)_3(VO_4)_2O$ (A = Li, Na) [27], $A(UO_2)_4(VO_4)_3$ (A = Li, Na) [28] and $A_3(UO_2)_7(VO_4)_5O$ (A = Li, Na, Ag) [29]. The uranyl vanadate frameworks release perpendicular non-crossing channels occupied by the monovalent cations. These vanadates are built from perpendicular $^1_\infty[UO_5]^{4-}$ chains connected by two types of uranyl vanadate layers with autunite sheet anion-topology [30,31] common to many layered phosphates but never met in vanadates.

In this paper, we report the synthesis, the crystal structure determination and the electrical conductivity properties of three new lithium uranyl phosphates: $Li_2(UO_2)_3(PO_4)_2O$, $Li(UO_2)_4(PO_4)_3$ and $Li_3(UO_2)_7(PO_4)_5O$ with three-dimensional structures.

2. Experimental

2.1. Synthesis

$Li_2(UO_2)_3(PO_4)_2O$ (**1**) and $Li(UO_2)_4(PO_4)_3$ (**2**) powders were prepared by solid state reaction. The reactants, uranium oxide, U_3O_8, ammonium hydrogenophosphate, $(NH_4)_2HPO_4$ and lithium carbonate, Li_2CO_3, were weighted in stœchiometric proportions. The mixtures were ground in an agate mortar and heated in gold containers. After successive 24 h heating treatments at 300, 500 and 650 °C, the mixtures were maintained at 850 °C during seven days with daily intermediate grindings at room temperature. The attempts of powder synthesis of $Li_3(UO_2)_7(PO_4)_5O$ **(3)**, following the same process, systematically gave a mixture of the three compounds **1**, **2** and **3**.

Single crystals were obtained by melting the synthesized powders of **1** and **2** composition in platinum crucibles at 1100 °C, the furnace was then slowly cooled at 5 °C/h. The melting of the lithium uranyl phosphates are non-congruent, nevertheless, yellow single crystals of **1**, **2** and **3** could be isolated from each melted mixture.

2.2. Powder X-ray diffraction

The powder X-ray diffraction patterns of **1** and **2** were recorded using a D8 Advance Bruker diffractometer with Cu$K\alpha$ radiation and an energy dispersive detector (sol-X), over a 2θ range of 10°–80° at 0.02° increments. High temperature X-ray diffraction on **1** and **2** was carried out at 450 °C using a Bruker D8 diffractometer equipped with a Anton Paar HTK 1200N high temperature device, with a Cu$K\alpha$ radiation and a Vantec 1 linear detector (2θ range: 10°–50°, 0.015° increments). The profile fitting and the cell parameters refinements were performed using the powder option of JANA2000 [32].

2.3. Single crystal X-ray diffraction

For the three compounds, a single crystal was mounted on a glass fibre and aligned on a Bruker X8 Apex II CCD 4 K diffractometer. The X-rays intensity data were collected at room temperature using Mo$K\alpha$ radiation ($\lambda = 0.71073$ Å) selected by a graphite monochromator. The raw data frames were integrated with SAINT program [33], which also applies corrections for Lorentz and polarization effects. A semi-empirical absorption correction was applied using the program SADABS [34], based on redundancy. **1** and **3** crystallize in the tetragonal system with $a = 7.1109(2)$ Å, $c = 25.0407(8)$ Å and $a = 9.9305(2)$ Å, $c = 14.5741(3)$ Å, respectively. The monoclinic P Bravais lattice of **2**, $a = 9.8829(2)$ Å, $b = 9.8909(2)$ Å, $c = 17.4871(4)$ Å and $\beta = 106.198(1)°$, displays an orthorhombic B pseudo-symmetry. The transformation of the monoclinic cell through the (100, 010, 102) matrix gives: $a = 9.8829$ Å, $b = 9.8902$ Å, $c = 33.586$ Å and $\beta = 89.78°$. But the averaging agreement factor in the orthorhombic cell, $R_{int} = 0.0848$, clearly dismiss this hypothesis. Thus, the structure of **2** was solved in the $P2_1/c$ space group. The position of the heaviest atoms (U and P) was determined by direct method using SIR97 [35], and then refined on $|F|$ using JANA2000 [32], the oxygen then lithium atoms were localized on Fourier difference maps. The crystallographic and experimental details are summarized in Table 1. The bond valences were calculated with the commonly used empirical expression $v_{ij} = \exp[(R_{ij} - d_{ij})/b]$ where d_{ij} is the distance between two atoms i and j, R_{ij} is the bond valence parameter [36], b is a constant equal 0.37 Å [37] except for U–O bonds for which $b = 0.519$ Å and $R_{ij} = 2.051$ Å coordination-independent parameters were taken from Burns et al. [38].

2.4. Electrical conductivity and thermal analysis

For the conductivity measurements, cold pressed cylindrical pellets of **1** and **2** powders were sintered at 900 °C and gold was deposited onto the two opposite circular sides. The measurements were performed by AC impedance spectroscopy over a temperature range from 200 to 800 °C, with a 20 °C increment. Each impedance set was recorded after one hour temperature stabilization.

The thermal stability of **1** and **2** was studied by differential scanning calorimetry performed with a DSC Setaram 141 instrument from room temperature to 1100 °C under air.

3. Results and discussion

The three structures are based on three-dimensional frameworks built from UO_7 pentagonal bipyramids, UO_6 square

Table 1
Crystallographic data and experimental details for structure determination of the three uranyl phosphates **1**, **2** and **3**.

Crystal data	**1**	**2**	**3**
Formula	$Li_2(UO_2)_3(PO_4)_2O$	$Li(UO_2)_4(PO_4)_3$	$Li_3(UO_2)_7(PO_4)_5O$
Formula molar weight	1029.9	1372	2401.9
Z	4	4	2
Unit cell dimensions			
a (Å)	7.1109(2)	9.8829(2)	9.9305(2)
b (Å)		9.8909(2)	
c (Å)	25.0407(8)	17.4871(4)	14.5741(3)
β (°)		106.198(1)	
V (Å^3)	1266.2(1)	1641.55(8)	1437.21(7)
Space group	$I4_1/amd$ (no. 141)	$P2_1/c$ (no. 14)	$P\bar{4}2_1m$ (no. 113)
Calculated density	5.403(1)	5.550(1)	5.548(1)
Data collection			
Theta range (deg)	2.98–30.51	2.15–30.57	2.48–43.88
Indices range	$-10\leqslant h\leqslant 7$; $-10\leqslant k\leqslant 9$; $-35\leqslant l\leqslant 34$	$-14\leqslant h\leqslant 14$; $-14\leqslant k\leqslant 14$; $-24\leqslant l\leqslant 24$	$-18\leqslant h\leqslant 18$; $-18\leqslant k\leqslant 18$; $-28\leqslant l\leqslant 24$
Reflections collected	7337	33382	46418
Reflections observed	5914	24167	35355
Independent reflections	561	5021	5576
Independent reflections observed	479	4201	4527
Criterion for observation	$I>3\sigma(I)$	$I>3\sigma(I)$	$I>3\sigma(I)$
$F000$	1728	2303	2016
R_{int}	0.0604	0.0356	0.0763
Refinement			
Data/restraints/parameters	561/0/38	5021/0/249	5576/0/137
Final R indices (R, wR) obs	0.0344, 0.0475	0.0216, 0.0314	0.0348, 0.0383
Final R indices (R, wR) all	0.0399, 0.0493	0.0304, 0.0336	0.0500, 0.0399
Extinction coefficient	0.118(9)	0.018(2)	0.130(3)

Table 2
Refined atomic coordinates and equivalent isotropic displacement parameters for $Li_2(UO_2)_3(PO_4)_2O$ (**1**).

Atom	Wick.	Occ.	x	y	z	$U_{eq.}$
U(1)	4*b*	1	0	0.25	0.375	0.0121(2)
U(2)	8*e*	1	0.5	0.75	0.29129(2)	0.0104(2)
P(1)	8*e*	1	0	0.75	0.3374(2)	0.0104(9)
O(1)	16*h*	1	0	0.922(1)	0.3731(2)	0.015(2)
O(2)	16*h*	1	0.8326(9)	0.75	0.2985(2)	0.014(2)
O(3)	8*e*	1	0	0.25	0.3054(4)	0.019(3)
O(4)	16*h*	1	0.5	0.4981(9)	0.2871(2)	0.021(2)
O(5)	4*a*	1	0.5	0.75	0.375	0.037(6)
Li(1)	8*e*	1	0.5	0.25	0.307(2)	0.039(8)

Table 3
Anisotropic displacement parameters of all atoms except lithium for $Li_2(UO_2)_3(PO_4)_2O$ (**1**).

Atom	U_{11}	U_{22}	U_{33}	U_{12}	U_{13}	U_{23}
U(1)	0.0111(3)	0.0111(3)	0.0140(5)	0	0	0
U(2)	0.0101(3)	0.0136(3)	0.0076(4)	0	0	0
P(1)	0.010(2)	0.012(2)	0.009(2)	0	0	0
O(1)	0.018(4)	0.013(3)	0.014(3)	0	0	−0.002(2)
O(2)	0.009(3)	0.026(4)	0.006(3)	0	−0.005(2)	0
O(3)	0.042(6)	0.019(5)	−0.003(4)	0	0	0
O(4)	0.033(4)	0.012(4)	0.018(3)	0	0	0.011(3)
O(5)	0.020(5)	0.020(5)	0.07(2)	0	0	0

bipyramids and PO_4 tetrahedra that are edge and corner shared.

3.1. Structure of $Li_2(UO_2)_3(PO_4)_2O$ (**1**)

The structure of **1** was solved in the space group $I4_1/amd$. The refined atomic and anisotropic displacement parameters are reported in Tables 2 and 3, respectively. There are two symmetrically unique uranium atoms U(1) and U(2) in (4*b*) and (8*e*) sites, respectively. The two uranium atoms are strongly bonded to two oxygen atoms forming a linear uranyl cation $(UO_2)^{2+}$ for U(1) and a nearly linear uranyl ion for U(2) with a O(4)═U(2)═O(4) bond-angle of 173.2(3)° (Table 4). The O(3)═U(1)═O(3) uranyl ion is parallel to [001] and is surrounded in the equatorial plane by four symmetrically related O(1) atoms at 2.232(7) Å to form an $U(1)O_6$ square bipyramid. The U(2) coordination is completed in the equatorial plane by five oxygen atoms, one O(5) at a short distance, 2.0962(5) Å, and four O(2) at 2.372(6) (2*x*) and 2.544(6) Å (2*x*), to form an $U(2)O_7$ pentagonal bipyramid. The uranyl U═O distances are significantly shorter in the $U(1)O_6$ polyhedra (1.74(1) Å) than in the $U(2)O_7$ (1.794(6) Å). The unique P atom occupies a (8*e*) site and is tetrahedrally coordinated. The $U(1)O_6$ square bipyramids and PO_4 tetrahedra are connected by sharing vertices, each uranyl polyhedron is linked through its four equatorial oxygen atoms to four phosphate tetrahedra, and each tetrahedron is only connected to two uranium polyhedra resulting in $^2_\infty[(UO_2)(PO_4)_2]^{4-}$ layers (Fig. 1c), called hereafter S layers, parallel to (001) (Fig. 1e). The layers have the autunite sheet-anion topology (Fig. 1a) that contain only squares [30], in the autunite-type sheet $^2_\infty[(UO_2)(PO_4)]^-$ (Fig. 1b) common to many uranyl phosphates [1–3] half the squares are occupied, one quarter by UO_6 polyhedra and one quarter by XO_4 tetrahedra (X = P, As), thus the S layers can be deduced from the autunite layers by the removal of half the uranium polyhedra. The structure of $K_4(UO_2)(PO_4)_2$ contains the S layers connected through the interlayer K^+ cations [39]. The $U(2)O_7$ pentagonal bipyramids are connected together through opposite edges to create infinite

Table 4
Selected bond distances (Å) and angles (deg) for $Li_2(UO_2)_3(PO_4)_2O$ (**1**).

	Distance or angle	v_{ij}
U(1)–O(3)	1.74(1)	1.810
U(1)–O(3)v	1.74(1)	1.810
U(1)–O(1)i	2.332(7)	0.582
U(1)–O(1)ii	2.332(7)	0.582
U(1)–O(1)iii	2.332(7)	0.582
U(1)–O(1)iv	2.332(7)	0.582
		$\sum v_{ij} = 5.95$
U(2)–O(4)	1.794(6)	1.641
U(2)–O(5)	2.0962(5)	0.917
U(2)–O(2)	2.372(6)	0.539
U(2)–O(2)vii	2.372(6)	0.539
U(2)–O(2)vi	2.544(6)	0.387
U(2)–O(2)viii	2.544(6)	0.387
U(2)–O(4)ix	1.794(6)	1.641
		$\sum v_{ij} = 6.05$
O(3)–U(1)–O(3)v	180°	
P(1)–O(1)	1.515(7)	1.272
P(1)–O(1)iii	1.515(7)	1.272
P(1)–O(2)x	1.538(6)	1.195
P(1)–O(2)vii	1.538(6)	1.195
		$\sum v_{ij} = 4.93$
O(4)–U(2)–O(4)ix	173.2(3)°	
Li(1)–O(4)	1.83(2)	0.371
Li(1)–O(4)xi	1.83(2)	0.371
Li(1)–O(1)v	2.14(3)	0.162
Li(1)–O(1)iv	2.14(3)	0.162
		$\sum v_{ij} = 1.07$
O(1)v–Li(1)–O(1)iv	70(2)°	
O(1)–Li(1)–O(4)	4 × 102.8(9)°	
O(4)–Li(1)–O(4)xi	149(2)°	

Symmetry transformation applied to atoms: (i) $x,-1+y,z$; (ii) $-5/4+y,5/4-x,3/4-z$; (iii) $-x,3/2-y,z$; (iv) $5/4-y,1/4+x,3/4-z$; (v) $-1/4+y,5/4-x,3/4-z$; (vi) $3/2-x,3/2-y,1/2-z$; (vii) $1-x,y,z$; (viii) $-1/2+x,3/2-y,1/2-z$; (ix) $1-x,3/2-y,z$; (x) $-1+x,y,z$; (xi) $1-x,1/2-y,z$.

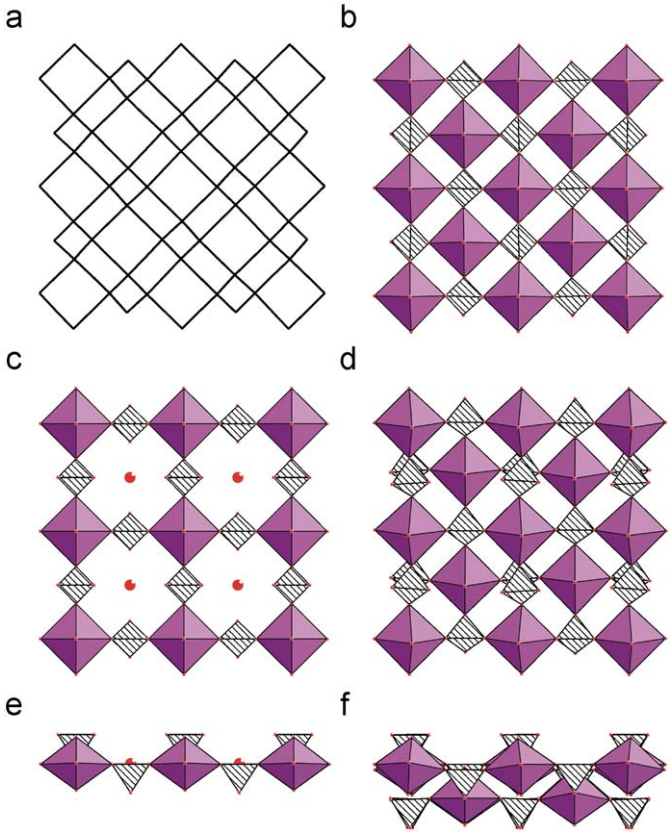

Fig. 1. All the squares of the autunite sheet anion-topology (a) are occupied in the autunite type sheet, one half by UO_6 polyhedra and one half by XO_4 tetrahedra (X = P, As) (b). In the S layer $^2_\infty[(UO_2)(PO_4)_2]^{4-}$, half the UO_6 polyhedra are removed (c). In the D layer $^2_\infty[(UO_2)_2(PO_4)_3]^{5-}$ each tetrahedra is replaced by two tetrahedra on each side of the sheet (d). For the S and D layers the PO_4 edges not involved in the sheet building are perpendicular above and below the sheet (e and f) and allow the hanging of perpendicular $^1_\infty[UO_5]^{4-}$ chain. In (d) the front view is slightly shifted to make visible all the PO_4 tetrahedra. Uranium octahedra are grey, phosphor tetrahedra are hatched. The isolated atoms is (c) and (e) are oxygen atoms shared between $^1_\infty[UO_5]^{4-}$ chains. (For interpretation of the references to color in the figure legend, the reader is referred to the web version of this article.)

$^1_\infty[UO_5]^{4-}$ chains (Fig. 2a). The PO_4 edges not involved in the S sheet building that are above the sheet are perpendicular to the PO_4 edges below the sheet allowing the linkage of perpendicular $^1_\infty[UO_5]^{4-}$ chains alternatively parallel to [100] and [010] resulting in a three-dimensional framework $^3_\infty[(UO_2)_3(PO_4)_2]^{2-}$ (Fig. 3a). The perpendicular $^1_\infty[UO_5]^{4-}$ chains are also connected together by the equatorial O(5) oxygen atoms, that occupy the position of the removed uranium in the autunite-type sheet, to create a three-dimensional uranium–oxygen framework (Fig. 2b). The equatorial U(2)–O(5) bond length is notably small, 2.0962(5) Å, compared to the U(2) mean equatorial distance, 2.386 Å in **1** and to the average distance of 2.34(10) Å determined from 125 UO_7 polyhedra [30]. So short distances have already been reported in equatorial corner shared uranyl polyhedra, which is a rather rare connectivity way, as for example in β-U_3O_8 with U–O = 2.117(16) Å [40], $K_4((UO_2)_5(TeO_3)_2O_5)$ with U–O = 2.105(1) Å [41] and $K_6((UO_2)_5(VO4)_2O_5)$ [42] with U–O = 2.12(1) Å. In **1**, this short distance is necessary to satisfy the valence of the O(5) atom which is calculated to 1.84 vu (valence unit). The only example of mineral compound containing $^1_\infty[UO_5]^{4-}$ chains running in two perpendicular directions is that of soddyite, $(UO_2)_2SiO_4 \cdot 2H_2O$ [43], where uranyl chains are connected through SiO_4 tetrahedra, the chains are not directly connected and the non-shared oxygen is then a water oxygen.

The uranyl phosphate framework creates nearly circular channels running along [100] and [010]. These tunnels can be described from face-shared O_6 octahedra of uranyl oxygen atoms only (Fig. 4a). The Li^+ ions do not occupy the centre of the channels, that is to say the centre of the octahedron but are displaced towards the border of the tunnels at the middle of the O(4)–O(4) edges. So the lithium atoms are bounded to four oxygen atoms at $2 \times 1.83(2)$ and $2 \times 2.14(3)$ Å forming a very distorted tetrahedron with O(1)–Li(1)–O(1), O(1)–Li(1)–O(4) and O(4)–Li(1)–O(4) angles of 70(2)°, 102.8(9)° and 148(2)°, respectively.

The bond valence sums calculated for U, P and Li are in good agreement with the expected valence, the +6, +5 and +1, respectively.

3.2. *Structure of $Li(UO_2)_4(PO_4)_3$* (**2**)

All the atoms of **2** occupy (4*e*) general positions of $P2_1/c$ space group. The refined atomic positions and displacement parameters are reported in Tables 5 and 6, respectively. There are four independent U atoms, three P atom sites, twenty oxygen ones and one independent lithium ion. The four U atoms form UO_2^{2+} uranyl units, with six uranyl bond lengths in a narrow range from 1.742(4) to 1.767(4) Å and two longer for U(1) and U(2) at 1.875(4) and 1.871(4) Å, respectively, and O–U–O angles varying from 178.3(2)° to 179.5(2)° (Table 7). The U atoms coordination is

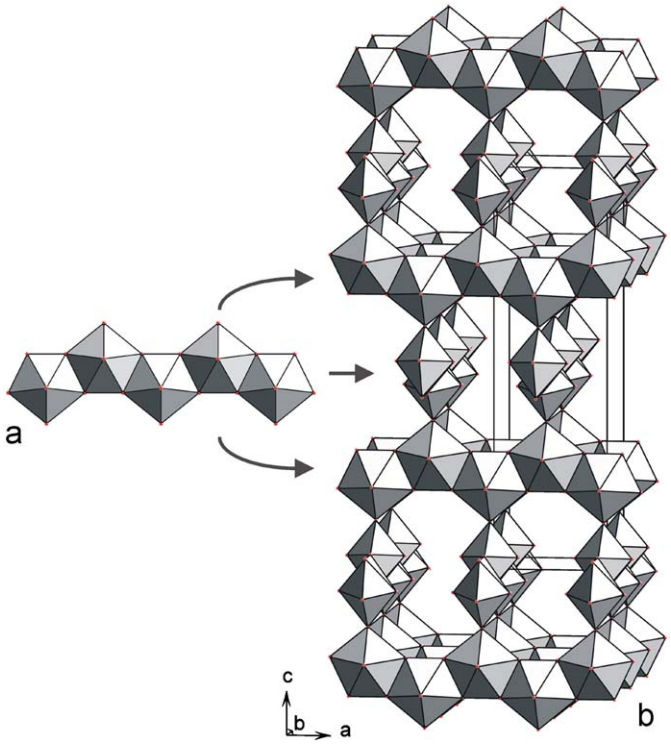

Fig. 2. The $^{1}_{\infty}[UO_5]^{4-}$ chains of edge-shared UO_7 pentagonal bipyramids common to the three compounds (a) are connected through the non-shared oxygen atoms to built a uranium oxygen framework in $Li_2(UO_2)_3(PO_4)_2O$ (**1**) (b).

completed in the equatorial plane by four oxygen atoms for U(1) and U(2) atoms to a square bipyramid and by five oxygen atoms for U(3) and U(4) to a pentagonal bipyramid. The P atoms are at the centre of slightly distorted PO_4 tetrahedra. A $P(1)O_4$ tetrahedron shares its four vertices with equatorial oxygen atoms of two $U(1)O_6$ and two $U(2)O_6$ square bipyramids. A $P(2)O_4$ tetrahedron shares two corners with two $U(2)O_6$ polyhedra and a $P(3)O_4$ tetrahedron two corners with two $U(1)O_6$ polyhedra. This linkage of PO_4 tetrahedra and UO_6 square bipyramids forms a

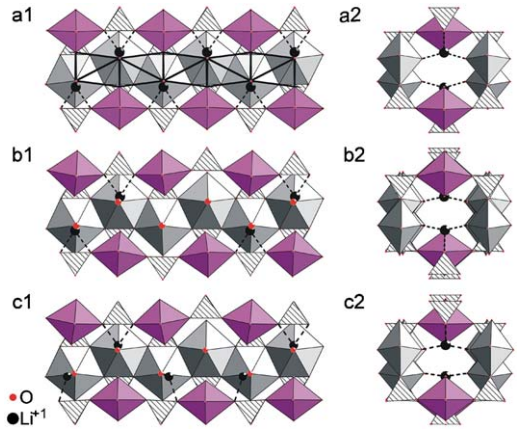

Fig. 4. Lithium coordination and distribution along the channels in $Li_2(UO_2)_3(PO_4)_2O$ (a1), $Li(UO_2)_4(PO_4)_3$ (b1) and $Li_3(UO_2)_7(PO_4)_5O$ (c1), a2, b2 and c2 display the corresponding perpendicular views. The channels are delimited by uranyl oxygen atoms forming face shared octahedra (black edges, a1).

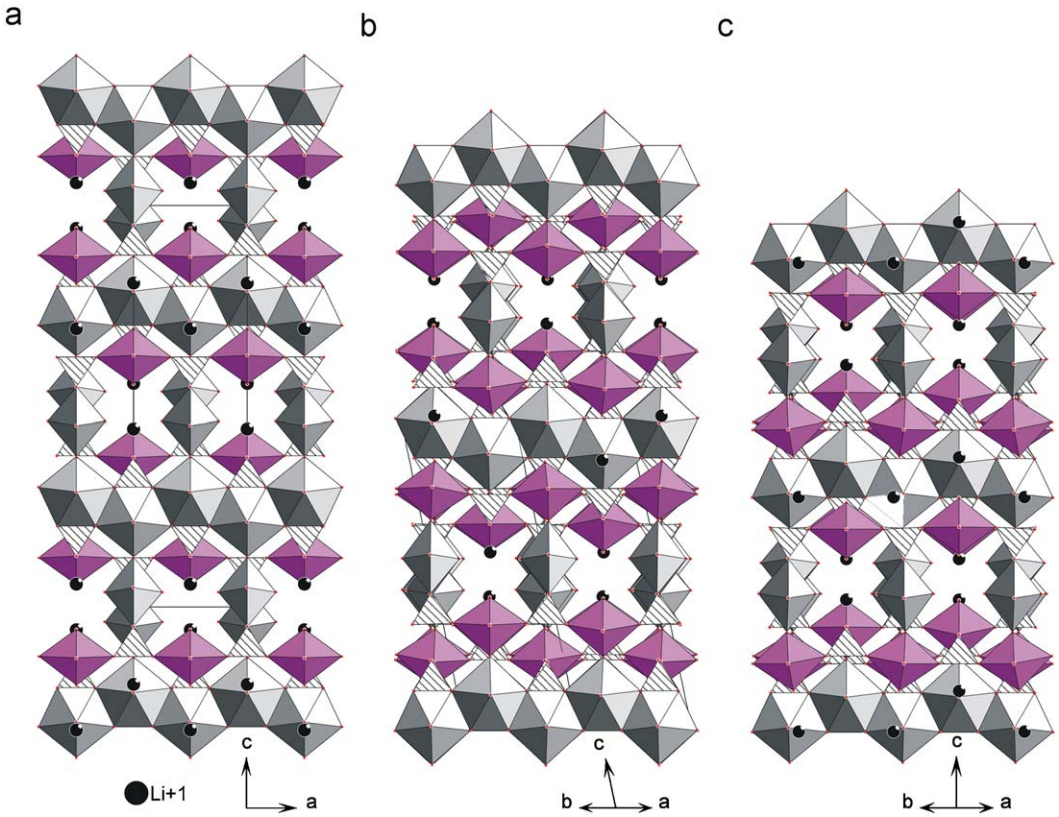

Fig. 3. Crystal structures of $Li_2(UO_2)_3(PO_4)_2O$ (a), $Li(UO_2)_4(PO_4)_3$ (b) and $Li_3(UO_2)_7(PO_4)_5$ (c) showing the three-dimensional frameworks built by corner or edge sharing of UO_6 square bipyramids (light grey), UO_7 pentagonal bipyramids (medium grey) and PO_4 tetrahedra (hatched).

Table 5
Refined atomic coordinates and equivalent isotropic displacement parameters for $Li(UO_2)_4(PO_4)_3$ (**2**).

Atom	Wick.	Occ.	x	y	z	$U_{eq.}$
U(1)	4*e*	1	0.53168(2)	0.12533(2)	0.31155(2)	0.00589(6)
U(2)	4*e*	1	0.97181(2)	0.12330(2)	0.19176(2)	0.00567(6)
U(3)	4*e*	1	0.08649(2)	0.13514(2)	0.44337(2)	0.00846(6)
U(4)	4*e*	1	0.39381(2)	0.11471(2)	0.05782(1)	0.00842(6)
P(1)	4*e*	1	0.25480(1)	0.8747(2)	0.25740(8)	0.0097(4)
P(2)	4*e*	1	0.6929(2)	0.8779(2)	0.13169(8)	0.0063(4)
P(3)	4*e*	1	0.1884(2)	0.3725(2)	0.13248(8)	0.0064(4)
O(1)	4*e*	1	0.2340(4)	0.2790(4)	0.0732(2)	0.013(2)
O(2)	4*e*	1	0.7996(4)	0.9718(4)	0.1838(2)	0.017(2)
O(3)	4*e*	1	0.1971(4)	0.7877(4)	0.3142(2)	0.017(2)
O(4)	4*e*	1	0.0771(4)	0.4589(4)	0.0731(2)	0.013(2)
O(5)	4*e*	1	0.7562(4)	0.8029(4)	0.0726(2)	0.014(2)
O(6)	4*e*	1	0.5904(4)	0.1319(4)	0.4166(2)	0.020(2)
O(7)	4*e*	1	0.3699(4)	0.9621(4)	0.3142(2)	0.016(2)
O(8)	4*e*	1	0.1216(4)	0.2913(4)	0.1849(2)	0.016(2)
O(9)	4*e*	1	0.6309(4)	0.7820(4)	0.1783(2)	0.015(2)
O(10)	4*e*	1	0.5766(4)	0.9599(4)	0.0723(2)	0.015(2)
O(11)	4*e*	1	0.0162(4)	0.1314(4)	0.3029(2)	0.015(2)
O(12)	4*e*	1	0.4659(4)	0.1140(4)	0.2003(3)	0.016(2)
O(13)	4*e*	1	0.3082(4)	0.4583(4)	0.1789(2)	0.014(2)
O(14)	4*e*	1	0.3182(4)	0.7857(4)	0.2059(2)	0.016(2)
O(15)	4*e*	1	0.9278(4)	0.1157(4)	0.0873(2)	0.022(2)
O(16)	4*e*	1	0.5143(4)	0.2460(4)	0.0575(2)	0.019(2)
O(17)	4*e*	1	0.1403(4)	0.9644(4)	0.2070(2)	0.017(2)
O(18)	4*e*	1	−0.0448(4)	0.2531(4)	0.4432(3)	0.021(2)
O(19)	4*e*	1	0.2185(4)	0.0146(4)	0.4435(2)	0.019(2)
O(20)	4*e*	1	0.2757(4)	−0.0158(4)	0.0583(3)	0.021(2)
Li(1)	4*e*	1	0.329(2)	0.873(2)	0.419(2)	0.064(4)

Table 6
Anisotropic displacement parameters of all atoms except for Li for $Li(UO_2)_4(PO_4)_3$ (**2**).

Atom	U_{11}	U_{22}	U_{33}	U_{12}	U_{13}	U_{23}
U(1)	0.00601(9)	0.0065(1)	0.0049(2)	0.00009(6)	0.00104(7)	−0.00007(6)
U(2)	0.00597(9)	0.0066(1)	0.0041(1)	−0.00025(6)	0.00088(7)	−0.00005(6)
U(3)	0.0098(1)	0.0106(1)	0.0045(1)	−0.00413(6)	0.00131(7)	−0.00033(7)
U(4)	0.0092(1)	0.0105(1)	0.0047(1)	0.00391(6)	0.00061(7)	−0.00034(7)
P(1)	0.0085(6)	0.0078(6)	0.0132(7)	0.0001(4)	0.0037(5)	−0.0008(4)
P(2)	0.0068(5)	0.0094(6)	0.0023(6)	0.0001(4)	0.0006(5)	−0.0003(4)
P(3)	0.0076(6)	0.0074(6)	0.0036(6)	−0.0002(4)	0.0005(5)	0.0000(4)
O(1)	0.015(2)	0.019(2)	0.004(2)	0.012(2)	0.001(2)	0.001(2)
O(2)	0.023(2)	0.015(2)	0.013(2)	−0.009(2)	0.005(2)	−0.000(2)
O(3)	0.015(2)	0.014(2)	0.023(2)	−0.008(2)	0.007(2)	−0.003(2)
O(4)	0.017(2)	0.017(2)	0.002(2)	0.012(2)	−0.001(2)	0.001(2)
O(5)	0.019(2)	0.015(2)	0.007(2)	0.011(2)	0.004(2)	−0.002(2)
O(6)	0.026(2)	0.026(2)	0.005(2)	0.005(2)	−0.003(2)	−0.003(2)
O(7)	0.017(2)	0.014(2)	0.019(2)	−0.006(2)	0.007(2)	−0.001(2)
O(8)	0.016(2)	0.019(2)	0.012(2)	−0.009(2)	0.003(2)	0.000(2)
O(9)	0.017(2)	0.018(2)	0.009(2)	−0.007(2)	0.002(2)	−0.001(2)
O(10)	0.020(2)	0.021(2)	0.003(2)	0.015(2)	0.000(2)	0.002(2)
O(11)	0.018(2)	0.017(2)	0.009(2)	−0.004(2)	0.003(2)	−0.003(2)
O(12)	0.018(2)	0.015(2)	0.014(2)	0.000(2)	0.003(2)	−0.001(2)
O(13)	0.015(2)	0.017(2)	0.009(2)	−0.009(2)	0.001(2)	−0.001(2)
O(14)	0.016(2)	0.019(2)	0.014(2)	0.006(2)	0.004(2)	−0.003(2)
O(15)	0.030(2)	0.030(2)	0.004(2)	−0.005(2)	0.003(2)	−0.000(2)
O(16)	0.019(2)	0.025(2)	0.012(2)	−0.005(2)	0.001(2)	−0.003(2)
O(17)	0.015(2)	0.016(2)	0.019(2)	0.008(2)	0.003(2)	−0.001(2)
O(18)	0.017(2)	0.023(2)	0.020(2)	0.008(2)	−−0.001(2)	0.000(2)
O(19)	0.019(2)	0.019(2)	0.020(2)	0.005(2)	0.006(2)	−0.002(2)
O(20)	0.021(2)	0.019(2)	0.023(2)	−0.006(2)	0.005(2)	0.001(2)

$^2_\infty[(UO_2)_2(PO_4)_3]^{5-}$ layer parallel to (001) (Fig. 1d) called D layer. These layers are related to the autunite-type layer by replacing one half of the tetrahedra by two tetrahedra on each side of the mean plane of the layer, these two tetrahedra have edges no involved in the layer formation that are perpendicular one to the other are further shared with $^1_\infty[UO_5]^{4-}$ chains built by edge-sharing of $U(3)O_7$ and $U(4)O_7$ pentagonal bipyramids, then the two chains hanged on each side of a layer are perpendicular. Two perpendicular $^1_\infty[UO_5]^{4-}$ chains are moved away by the

Table 7
Selected bond distances (Å) and angles (°) for $Li(UO_2)_4(PO_4)_3$ (**2**).

	Distance or angle	v_{ij}
U(1)–O(6)	1.767(4)	1.728
U(1)–O(12)	1.875(4)	1.404
U(1)–O(14)ii	2.250(4)	0.682
U(1)–O(13)ii	2.261(4)	0.667
U(1)–O(9)ii	2.275(4)	0.649
U(1)–O(7)i	2.282(4)	0.641
		$\sum v_{ij} = 5.77$
U(2)–O(15)	1.757(4)	1.762
U(2)–O(11)iii	1.871(4)	1.415
U(2)–O(2)i	2.243(4)	0.691
U(2)–O(8)iii	2.251(4)	0.680
U(2)–O(17)iv	2.251(4)	0.680
U(2)–O(3)ii	2.312(4)	0.605
		$\sum v_{ij} = 5.84$
O(6)–U(1)–O–(12)	178.3(2)°	
U(3)–O(18)	1.745(4)	1.803
U(3)–O(19)	1.767(4)	1.728
U(3)–O(4)vi	2.340(4)	0.573
U(3)–O(5)ii	2.343(4)	0.570
U(3)–O(11)	2.360(4)	0.551
U(3)–O(4)v	2.478(4)	0.439
U(3)–O(1)v	2.481(3)	0.437
		$\sum v_{ij} = 6.10$
O(11)–U(2)–O(15)	179.1(2)°	
U(4)–O(20)	1.742(4)	1.814
U(4)–O(16)	1.763(4)	1.742
U(4)–O(10)i	2.327(4)	0.588
U(4)–O(1)	2.333(4)	0.581
U(4)–O(12)	2.392(4)	0.518
U(4)–O(5)vii	2.485(3)	0.433
U(4)–O(10)vii	2.486(4)	0.433
		$\sum v_{ij} = 6.11$
O(18)–U(3)–O(19)	179.5(2)°	
P(1)–O(14)	1.515(5)	1.272
P(1)–O(17)	1.512(4)	1.282
P(1)–O(3)	1.539(5)	1.192
P(1)–O(7)	1.548(4)	1.163
		$\sum v_{ij} = 4.91$
O(16)–U(4)–O(20)	179.5(2)	
P(2)–O(9)	1.489(4)	1.365
P(2)–O(2)	1.506(4)	1.303
P(2)–O(5)	1.539(4)	1.192
P(2)–O(10)	1.547(4)	1.167
		$\sum v_{ij} = 5.03$
P(3)–O(13)	1.498(4)	1.332
P(3)–O(8)	1.503(5)	1.314
P(3)–O(4)	1.543(4)	1.179
P(3)–O(1)	1.547(4)	1.167
		$\sum v_{ij} = 4.99$
Li(1)–O(19)ix	1.89(2)	0.314
Li(1)–O(16)viii	1.95(2)	0.269
Li(1)–O(3)	2.10(2)	0.153
Li(1)–O(7)	2.16(2)	0.180
		$\sum v_{ij} = 0.92$

Symmetry transformation applied to atoms: (i) $x,-1+y,z$; (ii) $1-x,-1/2+y,1/2-z$; (iii) $1+x,y,z$; (iv) $1+x,-1+y,z$; (v) $x,1/2-y,1/2+z$; (vi) $-x,-1/2+y,1/2-z$; (vii) $1-x,1-y,-z$; (viii) $1-x,1/2+y,1/2-z$; (ix) $x,1+y,z$.

presence of a D layer and cannot therefore be linked together any more by the oxygen atoms not involved in the chain formation. In fact in **2** these equatorial oxygen atoms are also uranyl oxygen atoms of the UO_6 square bipyramids, thus $U(1)O_6$ and $U(4)O_7$, on one hand, and $U(2)O_6$ and $U(3)O_7$, on the other, are directly connected through a so-called cation–cation interaction [44] involving O(12) and O(11) atoms, respectively. This double role of common oxygen could explain the rather long U(1)–O(11) and U(2)–O(12) uranyl bonds, 1.865(4) and 1.862(4) Å, respectively. Rather common in NpO_2^+ containing compounds, cation–cation interactions are rare in compounds that exclusively contain uranium in the form of uranyl cations. However in $(NH_4)_3(H_2O)_2[(UO_2)_{10}O_{10}(OH)][(UO_4)(H_2O)_2]$ [45], three equatorial oxygens of the UO_7 polyhedra that pillar the β-U_3O_8 type sheet are uranyl oxygens of uranium polyhedra forming the sheet at distances from the uranium centre between 1.90(2) and 2.00(2) Å. U═O distances of 1.86(4) and 1.829(7) Å involving a shared oxygen are observed in $Li_2(UO_2)_4(WO_4)_4O$ [46] and $Cs[(UO_2)_3(HIO_6)_2(OH)O(H_2O)]\cdot 1.5H_2O$ [47], respectively. The U–O equatorial distances with the bridging oxygen vary in the range 2.32–2.42 Å and are in the limits of the U–O equatorial distances generally observed. By contrast, in the uranium polyhedra zig-zag chains built on corner sharing pentagonal bipyramids connected through cation–cation interactions formed in UV_2O_8 [24], UO_2XO_4 (X = Mo [48], S or Se [49]) and UO_2Cl_2 [50], the uranyl bond length has an usual value in the range 1.79–1.81 Å whereas the equatorial U–O bond is quite long (around 2.5 Å) so as to compensate the bond valence. The bond valence sums calculation for cations in **2** gives, as a consequence of the relatively long uranyl bonds for oxygen atoms that participate to the cation–cation interactions, low values for the six coordinated U(1) and U(2), 5.77 and 5.84 vu, respectively. For the other atoms, the values are close to the theoretical valences, +6 for seven-coordinated U, +5 for P and +1 for Li (Table 7). The three-dimensional framework of **2** creates channels alternatively oriented along [110] and [1$\bar{1}$1] (Fig. 3b). In the same way than in **1**, the lithium cations are in the border of the channels, they are ordered on half of the possible positions along the channels (Fig. 4b), and are coordinated by a distorted tetrahedron of oxygen atoms. The alkaline cations slightly distort the chains repelling the two pentagonal bipyramids around them, O(16)–O(19) = 3.749(6) Å. Therefore, in the tunnels on both sides, the distance between pentagonal bipyramid uranyl vertices is reduced, O(18)–O(20) = 3.225(6) Å and the site is unoccupied (Fig. 5b). This distortion leads to a weak undulation of the $^1_\infty[UO_5]^{4-}$ chains, as a result, $U(1)O_6$ and $U(2)O_6$ octahedra, sharing one uranyl oxygen atom with the chains, are tilted out of the $^2_\infty[(UO_2)_2(PO_4)_3]^{5-}$ layer plane.

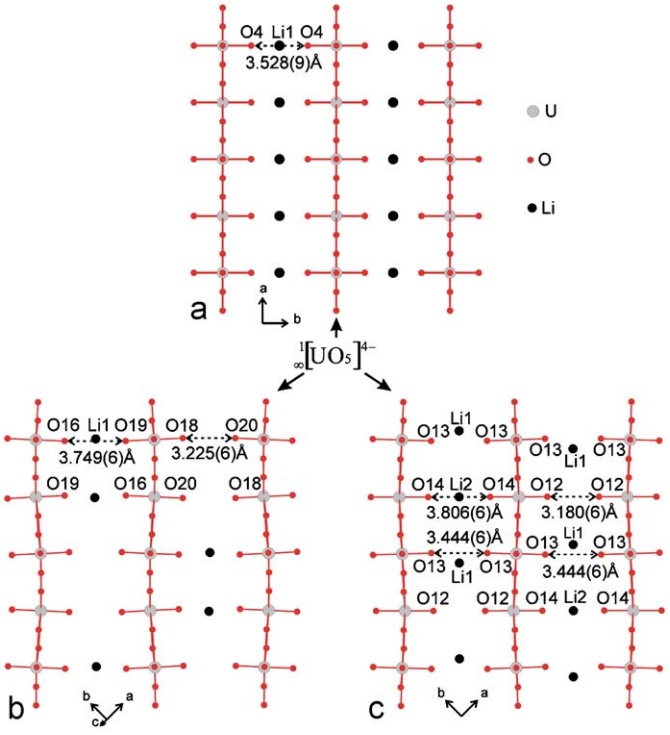

Fig. 5. Displacement of the lithium atoms and distortion of the channels in $Li_2(UO_2)_3(PO_4)_2O$ (a), $Li(UO_2)_4(PO_4)_3$ (b) and $Li_3(UO_2)_7(PO_4)_5O$ (c).

3.3. Structure of $Li_3(UO_2)_7(PO_4)_5O$ (**3**)

This compound crystallizes with $P\bar{4}21m$ symmetry. The refined positional and atomic displacement parameters are reported in Tables 8 and 9, respectively. The four crystallographically unique uranium atoms are part of uranyl ions, two of which, U(1) and U(4) occupying (2*c*) and (4*e*) sites, respectively, are in square bipyramidal environments and the two others, U(2) in (4*d*) and U(3) in (4*e*) sites, are in pentagonal bipyramidal environments. The phosphorus atoms are in (4*d*), (4*e*) and (2*c*) sites and the phosphate units are approximately tetrahedral. There are fifteen oxygen sites and two independent lithium atoms. The sharing of corners between $U(1)O_6$ square bipyramids and $P(2)O_4$ tetrahedra build $^2_\infty[(UO_2)(PO_4)_2]^{4-}$ layers similar to the S layers of **1**. The $U(4)O_6$ polyhedra are corner shared to $P(3)O_4$ and $P(1)O_4$ tetrahedra and create $^2_\infty[(UO_2)_2(PO_4)_3]^{5-}$ layers similar to the D layers in **2**. The S and D layers are stacked along [001] with the sequence S–D–S–D (Fig. 3c) and are connected through mutually perpendicular $^1_\infty[UO_5]^{4-}$ chains built from edge-shared $U(2)O_7$ and $U(3)O_7$ pentagonal bipyramids. These chains connect the layers by sharing edges with $P(2)O_4$ and $P(1)O_4$ tetrahedra of S and D layers, respectively. As in **1**, the chains on each side of the S layers are connected together by sharing O(15) equatorial vertices and the O(15) oxygen atom that belong to two U(2) uranium polyhedra participates to a short U–O equatorial bond, 2.0970(3) Å. As in **2**, the O(10) oxygen atom is involved in both a rather long U(4) uranyl bond, 1.862(6) Å, and an U(3) equatorial bond participating

Table 8
Refined atomic coordinates and equivalent isotropic displacement parameters for $Li_3(UO_2)_7(PO_4)_5O$ (**3**).

Atom	Wick.	Occ.	*x*	*y*	*z*	$U_{eq.}$
U(1)	2*c*	1	0	0.5	0.01069(3)	0.00466(7)
U(2)	4*d*	1	0	0	0.14388(2)	0.00359(6)
U(3)	4*e*	1	0.262262)	0.76226(2)	0.27987(2)	0.00339(5)
U(4)	4*e*	1	0.24833(2)	0.74833(2)	0.56959(2)	0.00167(5)
P(1)	4*d*	1	0	0	0.3648(1)	0.0017(4)
P(2)	4*e*	1	0.2541(2)	0.7541(2)	0.0623(2)	0.0043(4)
P(3)	2*c*	1	0.5	0	0.5129(2)	0.0047(4)
O(1)	4*e*	1	0.3375(4)	0.8375(4)	−0.0040(5)	0.014(2)
O(2)	4*e*	1	0.1641(4)	0.6641(4)	0.0044(5)	0.012(2)
O(3)	4*e*	1	0.5870(4)	0.0870(4)	0.5790(4)	0.013(2)
O(4)	8*f*	1	0.0918(4)	−0.0778(4)	0.2982(3)	0.0083(9)
O(5)	8*f*	1	0.3401(4)	0.6729(4)	0.1303(3)	0.011(1)
O(6)	4*e*	1	0.2343(4)	0.7343(4)	0.6923(4)	0.017(2)
O(7)	8*f*	1	−0.0834(4)	−0.0960(4)	0.4226(3)	0.008(1)
O(8)	4*e*	1	0.5903(4)	0.9097(4)	0.4547(3)	0.011(2)
O(9)	2*c*	1	0	0.5	0.1301(5)	0.017(2)
O(10)	4*e*	1	0.2631(4)	0.7631(4)	0.4426(4)	0.010(1)
O(11)	2*c*	1	0	0.5	0.8888(5)	0.036(2)
O(12)	4*e*	1	0.3868(4)	0.8868(4)	0.2787(4)	0.014(2)
O(13)	8*f*	1	0.1230(4)	0.1318(4)	0.1487(3)	0.015(2)
O(14)	4*e*	1	0.1355(4)	0.6355(4)	0.2803(4)	0.012(1)
O(15)	2*a*	1	0	0	0	0.012(2)
Li(1)	4*e*	1	0.290(2)	0.210(2)	0.132(2)	0.063(7)
Li(2)	2*c*	1	0	0.5	0.305(2)	0.08(2)

Table 9
Anisotropic displacement parameters of all atoms except for lithium for $Li_3(UO_2)_7(PO_4)_5O$ (**3**).

Atom	U_{11}	U_{22}	U_{33}	U_{12}	U_{13}	U_{23}
U(1)	0.004821)	0.0048(2)	0.0044(2)	0.0010(2)	0	0
U(2)	0.0045(2)	0.0047(1)	0.0015(2)	0.0037(2)	0	0
U(3)	0.00363(6)	0.00363(6)	0.0029(2)	0.00242(8)	0.00070(5)	0.00070(5)
U(4)	0.00116(7)	0.00116(7)	0.0027(2)	0.00040(9)	0.00003(4)	0.00003(4)
P(1)	0.0026(6)	0.0019(6)	0.0008(7)	0.0003(6)	0	0
P(2)	0.0043(5)	0.0043(5)	0.0044(8)	0.0024(7)	0.0007(3)	0.0007(3)
P(3)	0.0030(6)	0.0030(6)	0.0082(9)	0.0010(7)	0	0
O(1)	0.012(2)	0.012(2)	0.017(3)	−0.007(2)	−0.002(2)	−0.002(2)
O(2)	0.012(2)	0.012(2)	0.011(3)	−0.008(2)	0.003(2)	0.003(2)
O(3)	0.008(2)	0.008(2)	0.025(3)	−0.003(2)	−0.004(2)	−0.004(2)
O(4)	0.014(2)	0.010(2)	0.001(2)	0.009(2)	0.002(2)	−0.002(2)
O(5)	0.015(2)	0.011(2)	0.007(2)	0.013(2)	−0.000(2)	0.001(2)
O(6)	0.023(2)	0.023(2)	0.004(3)	0.008(3)	0.010(2)	0.010(2)
O(7)	0.010(2)	0.008(2)	0.008(2)	−0.008(2)	0.004(2)	0.003(2)
O(8)	0.011(2)	0.011(2)	0.010(2)	0.007(2)	0.001(2)	−0.001(2)
O(9)	0.022(3)	0.022(3)	0.007(3)	0.004(4)	0	0
O(10)	0.012(2)	0.012(2)	0.006(2)	−0.002(2)	0.000(2)	0.000(2)
O(11)	0.055(5)	0.055(5)	−0.003(3)	0.035(6)	0	0
O(12)	0.018(2)	0.018(2)	0.006(2)	−0.008(2)	−0.001(2)	−0.001(2)
O(13)	0.016(2)	0.013(2)	0.017(2)	−0.013(2)	−0.001(2)	0.000(2)
O(14)	0.014(2)	0.014(2)	0.008(2)	−0.006(2)	0.001(2)	0.001(2)
O(15)	0.018(3)	0.018(3)	0.002(4)	0	0	0

Table 10
Selected bond distances (Å), angles (°) and bond valence for $Li_3(UO_2)_7(PO_4)_5O$ (**3**).

	Distance or angle	v_{ij}
U(1)–O(9)	1.741(8)	1.817
U(1)–O(11)iv	1.776(7)	1.699
U(1)–O(1)i	2.284(4)	0.638
U(1)–O(1)ii	2.284(4)	0.638
U(1)–O(2)	2.306(4)	0.612
U(1)–O(2)iii	2.306(4)	0.612
		$\sum v_{ij} = 6.02$
U(4)–O(6)	1.799(5)	1.625
U(4)–O(10)	1.862(6)	1.439
U(4)–O(8)xiv	2.247(4)	0.685
U(4)–O(7)xii	2.257(4)	0.672
U(4)–O(7)xiii	2.257(4)	0.672
U(4)–O(3)xi	2.317(4)	0.599
		$\sum v_{ij} = 5.69$
O(9)–U(1)–O(11)iv	180°	
U(2)–O(13)	1.791(4)	1.650
U(2)–O(13)v	1.791(4)	1.650
U(2)–O(15)	2.0970(3)	0.915
U(2)–O(5)vi	2.347(4)	0.565
U(2)–O(5)vii	2.347(4)	0.565
U(2)–O(4)v	2.546(4)	0.385
U(2)–O(4)	2.546(4)	0.385
		$\sum v_{ij} = 6.11$
O(6)–U(4)–O(10)	179.9(2)°	
U(3)–O(12)	1.749(4)	1.789
U(3)–O(14)	1.780(4)	1.686
U(3)–O(4)viii	2.337(4)	0.576
U(3)–O(4)ix	2.337(4)	0.576
U(3)–O(10)	2.372(6)	0.539
U(3)–O(5)	2.477(4)	0.440
U(3)–O(5)x	2.477(4)	0.440
		$\sum v_{ij} = 6.05$
O(13)–U(2)–O(13)v	175.5(2)°	
P(1)–O(7)	1.517(4)	1.265
P(1)–O(7)v	1.517(4)	1.265
P(1)–O(4)	1.540(4)	1.189
P(1)–O(4)v	1.540(4)	1.189
		$\sum v_{ij} = 4.91$
O(12)–U(3)–O(14)	179.6(3)°	
P(3)–O(8)xvi	1.526(4)	1.235
P(3)–O(8)xi	1.526(4)	1.235
P(3)–O(3)	1.556(5)	1.139
P(3)–O(3)xv	1.556(5)	1.139
		$\sum v_{ij} = 4.75$
P(2)–O(1)	1.518(6)	1.262
P(2)–O(2)	1.521(5)	1.251
P(2)–O(5)	1.536(4)	1.202
P(2)–O(5)x	1.536(4)	1.202
		$\sum v_{ij} = 4.91$
Li(1)–O(13)	1.85(2)	0.354
Li(1)–O(13)vi	1.85(2)	0.354
Li(1)–O(2)ii	2.09(2)	0.185
Li(1)–O(6)xvii	2.58(2)	0.049
Li(1)–O(1)ii	2.59(2)	0.048
		$\sum v_{ij} = 0.99$
Li(2)–O(14)	1.937(8)	0.280
Li(2)–O(14)iii	1.937(8)	0.280
Li(2)–O(3)xviii	2.09(3)	0.185
Li(2)–O(3)xix	2.09(3)	0.185
Li(2)–O(9)	2.55(4)	0.053
		$\sum v_{ij} = 0.98$

Symmetry transformation applied to atoms: (i) $-1+y,1-x,-z$; (ii) $1-y,x,-z$; (iii) $-x,1-y,z$; (iv) $x,y,-1+z$; (v) $-x,-y,z$; (vi) $1/2-y,1/2-x,z$; (vii) $-1/2+y,-1/2+x,z$; (viii) $x,1+y,z$; (ix) $1/2+y,1/2+x,z$; (x) $-1/2+y,1/2+x,z$; (xi) $1-x,1-y,z$; (xii) $1/2+x,1/2-y,1-z$; (xiii) $-y,1+x,1-z$; (xiv) $-1/2+x,3/2-y,1-z$; (xv) $1-x,-y,z$; (xvi) $x,-1+y,z$; (xvii) $1-y,x,1-z$; (xviii) $y,1-x,1-z$; (xix) $-y,x,1-z$.

to a cation–cation interaction (Table 10), and giving a low bond valence sum for U(4) (5.69 vu). The bond valence sum of P(3) atom is also underestimated, 4.75 vu, with a mean P(3)–O distance of 1.541(5) Å while P(1)–O and P(2)–O mean distances are 1.528(4) and 1.526(4) Å, respectively. This P(3) atom is located in the double layers and the $P(3)O_4$ tetrahedron shares all its vertices with the equatorial basis of an uranyl octahedra. The elongation of the P–O bonds, leading to low bond valence sum (BVS) was already observed in some uranyl phosphates with autunite-type structure, such as $Mg(UO_2)_2(PO_4)_2(H_2O)_{10}$ [51] (BVS = 4.72 vu) and $Na((UO_2)(PO_4))(H_2O)_3$ [1] (BVS = 4.78 vu) or in the uranyl phosphate with a S-type layered structure $K_4UO_2(PO_4)_2$ [39] (BVS = 4.54 vu).

The crystal structure of **3** can be considered as an intergrowth of those of **1** and **2**. Similar channels are created and the lithium ions are localized between octahedra uranyl vertices at the border of the tunnels. The alkaline cations are arranged on three consecutive sites on four (Fig. 4c). Li(2) is between uranyl oxygen vertices of a square and a pentagonal bipyramids, with an O(14)–Li(2)–O(14) angle of 159(2)°, whereas Li(1) is slightly shifted towards one of the $U(1)O_6$ octahedron vertex with a smaller O(13)–Li(1)–O(13) angle, 138(2)° (Fig. 5b). Thus, Li(1) is bounded to three oxygen atoms, with two short Li–O distances, 1.85(2) Å and a longer, 2.09(2) Å (Fig. 5c). This coordination is rather rare for the lithium ions but has already been reported in some Li-containing complexes [52,53]. Li(2) has the distorted tetrahedral coordination encountered in **1** and **2**. As in **2**, Li(2) cations shift the pentagonal bipyramids and the tunnel sites on

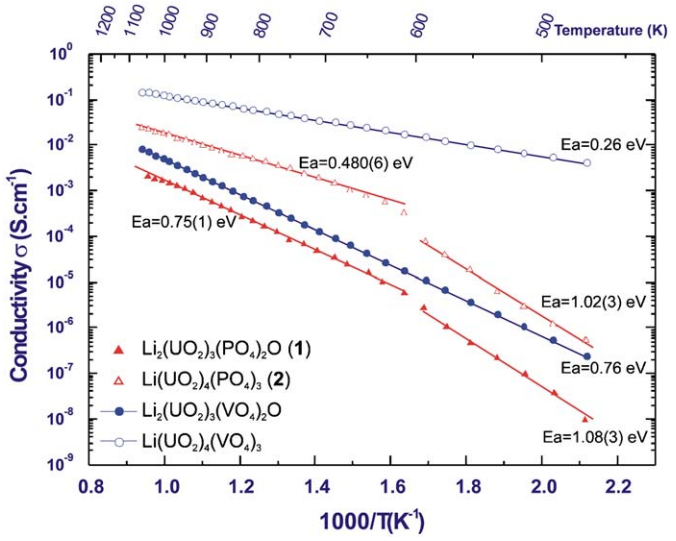

Fig. 6. Electrical conductivity of $Li_2(UO_2)_3(PO_4)_2O$ (a), $Li(UO_2)_4(PO_4)_3$ (b) and the vanadate analogous.

Table 11
Comparison of the phosphates and vanadates analogous.

X	$Li_2(UO_2)_3(XO_4)_2O$		$Li(UO_2)_4(XO_4)_3$		$Li_3(UO_2)_7(XO_4)_5O$	
	P	V	P	V	P	V
a (Å)	7.1109(2)	7.3303(5)	6.99(1)[a]	7.2379(5)	7.025(2)[a]	7.2794(9)
c (Å)	25.0407(8)	24.653(3)	33.586(1)[b]	33.677(2)	14.5741(3)	14.514(4)

[a] $a/\sqrt{2}$.
[b] $2c \cdot \sin \beta$.

either side are unoccupied. By contrast, Li(1) occupy all the sites along a line perpendicular to the channel (Fig. 6b). The short distance between the pentagonal bipyramid vertices requires the Li(1) cation to reduce the O(13)–Li(1)–O(13) angle to 138(2)°.

The three lithium uranyl phosphates **1**, **2** and **3** are built on frameworks similar to those reported in the recently published alkaline uranyl vanadates $A_2(UO_2)_3(VO_4)_2O$ [27], $A(UO_2)_4(VO_4)_3$ [28], $A_3(UO_2)_7(VO_4)_7O$ [29] (A = Li, Na). In the alkaline uranyl vanadates, the sodium ions occupy the centre of the octahedra forming the tunnels but the lithium cations are shifted toward the layers, as observed in the studied uranyl phosphates. In the vanadates, the monovalent cations are statistically distributed along the tunnels, with a site occupancy of 0.5 in $A(UO_2)_4(VO_4)_3$ and of 0.75 in $A_3(UO_2)_7(VO_4)_7O$. On contrast, in the phosphate analogous, the slight distortion of the tunnels by Li^+ ions forces them to fully occupy their sites. The smaller size of the phosphate tetrahedron compared to the VO_4 one causes a decrease of **1** and **2** cell parameters which are directly correlated to the layers dimensions. For the same reasons, the UO_7 bipyramid equatorial edges shared with the PO_4 tetrahedron are shortened, what generates a tightening of the corresponding O–U–O angle (55–56° in uranyl phosphates, 61°–63° in vanadates), an increase the $^1_\infty[UO_5]^{4-}$ chain width and therefore an increase of the **c** parameter. This explains why the c parameter is higher in $Li_2(UO_2)_3(PO_4)_2O$ than in $Li_2(UO_2)_3(VO_4)_2O$ (Table 11). By contrast, in $Li(UO_2)_4(XO_4)_3O$ (X = P, V) compounds, the c parameter of the phosphate is smaller than that of the vanadate. In these crystal structures, the $^1_\infty[UO_5]^{4-}$ chains are separated by the D layers. The distance between chains is imposed by the half height of UO_6 square bipyramids linked to the chain on one side, and by the height of PO_4 tetrahedron bounded to the chain on the other side. The c parameter is the sum of the chains width and D layer thickness. The increase of the first, in the uranyl phosphate, is compensated by the reduction of the latter. The differences between uranyl phosphates and uranyl vanadates are somewhat minor but they could explain the unsuccessful synthesis of hypothetical sodium or silver uranyl phosphates with the framework structures of **1**, **2** and **3**.

3.4. Electrical conductivity and thermal properties

The Arrhenius plots of the conductivity of **1** and **2** display a slope break at 600 K (Fig. 6). The differential thermal analysis curves did not evidence any phase transition. The high temperature (450 °C) powder X-ray patterns show a decrease of the cell parameters for both lithium uranyl phosphates and the diffraction peaks of **2** are narrower at high temperature, indicating a symmetry increase. The **1** and **2** cell parameters at high temperature were refined in the tetragonal system, the resulting values are: $a = 7.0269(7)$ Å $c = 24.797(3)$ Å, $V = 1224.4(2)$ Å^3 and $a = 9.7611(8)$ Å, $c = 33.372(2)$ Å, $V = 3179.7(4)$ Å^3, respectively. For the two compounds, the temperature increase induces a cell volume decrease of 3.2%, this evolution is inconsistent with the expected thermal expansion. A structural change may have caused the contraction of the cell. The most likely hypothesis is the shifting of lithium cations toward the centre of the tunnels. At room temperature, the lithium ions are in the border the channels, inducing a slight distortion of the $^1_\infty[UO_5]^{4-}$ chains for **2**. A shrinkage of the square (or quasi-square) cell basis is not compatible with the standing of the cations in these positions. Furthermore, the decrease of the activation energy above 600 K is in agreement with the hypothetical lithium position at the centre of the channel, which would make the cation mobility easier, Ea decreases from 1.02(3) to 0.480(6) eV for **2** and from 1.08(3) to 0.75(1) eV for **1**. The structural differences between lithium uranyl phosphates and vanadates affect the electrical conductivity (Fig. 6). The conductivity is lower and the activation energy is higher for the lithium phosphates than for the lithium uranyl vanadates analogous, $Ea = 0.27$ and 0.76 eV for $Li(UO_2)_4(VO_4)_3$ and $Li_2(UO_2)_3(VO_4)_2O$, respectively. This is explained by the smaller size of the tunnels in the phosphates and the statistical site occupancy in the vanadates. Above 600 K, the difference dwindles and the slope of the conductivity becomes equivalent for $Li_2(UO_2)_3(VO_4)_2O$ and $Li_2(UO_2)_3(PO_4)_2O$.

References

[1] A.J. Locock, P.C. Burns, M.J.M. Duke, T.M. Flynn, Can. Mineral. 42 (2004) 973–996.
[2] A.J. Locock, P.C. Burns, T.M. Flynn, Can. Mineral. 42 (2004) 1699–1718.
[3] A.J. Locock, P.C. Burns, T.M. Flynn, Can. Mineral. 43 (2005) 721–733.
[4] P. Piret, J. Piret-Meunier, Eur. J. Mineral. 3 (1) (1991) 69–77.
[5] P. Piret, M. Deliens, Bull. Minéral. 105 (1982) 125–128.
[6] A.J. Locock, P.C. Burns, J. Solid State Chem. 163 (2002) 275–280.
[7] J. Locock, A.J. Locock, P.C. Burns, J. Solid State Chem. 167 (2002) 226–236.
[8] A.J. Locock, P.C. Burns, Z. Kristallogr. 219 (2004) 259.
[9] S.A. Linde, Y.E. Gorbunova, A.V. Lavrov, A.B. Pobedina, Z. Neorg. Khim. 29 (1984) 1533–1537.
[10] S.A. Linde, Y.E. Gorbunova, A.V. Lavrov, V.G. Kuznetsov, Dokl. Akad. Nauk SSSR 242 (1978) 1083–1085.
[11] V.A. Sarin, S.A. Linde, L.E. Fikin, V.Ya. Dudarev, Yu.E. Gorbunova, Z. Neorg. Khim. 28 (1983) 1538–1541.
[12] E.V. Alekseev, S.V. Krivovitchev, T. Malcherek, W. Depmeier, J. Solid State Chem. 181 (2008) 3010–3015.
[13] P.B. Barton, Am. Miner. 43 (1958) 799–817.
[14] D.E. Appleman, H.T. Evans, J. Am. Miner. 50 (1965) 825–842.
[15] K. Mereiter, Neues Jahrb. Mineral. Monatsh 12 (1986) 552–560.
[16] P.G. Dickens, G.P. Stuttard, R.G.J. Ball, A.V. Powell, S. Hull, S. Patat, J. Mater.Chem. 2 (2) (1992) 161–166.
[17] F. Abraham, C. Dion, M. Saadi, J. Mater. Chem. 3 (5) (1993) 459–463.
[18] F. Abraham, C. Dion, N. Tancret, M. Saadi, Adv. Mater. Res. 1–2 (1994) 511–520.

[19] D.P. Shashkin, Dokl. Akad Nauk SSSR 220 (1975) 1410–1413.
[20] J. Borene, F. Cesbron, Bull. Soc. Fr. Mineral. Cristallogr. 93 (1970) 426–432.
[21] P. Piret, P. Declercq, D. Wauters-Stoop, Bull. Mineral. 103 (1980) 176–178.
[22] M. Rivenet, N. Vigier, P. Roussel, F. Abraham, J. Solid State Chem. 180 (2007) 722–733.
[23] N. Tancret, S. Obbade, F. Abraham, Eur. J. Solid State Inorg. Chem. 32 (1995) 195–207.
[24] A.M. Chippindale, P.G. Dickens, G.J. Flynn, G.P. Stuttard, J. Mater. Chem. 5 (1995) 141–146.
[25] M. Saadi, C. Dion, F. Abraham, J. Solid State Chem. 150 (2000) 72–80.
[26] S. Obbade, C. Dion, M. Saadi, F. Abraham, J. Solid State Chem. 177 (2004) 1567–1574.
[27] S. Obbade, L. Duvieubourg, C. Dion, F. Abraham, J. Solid State Chem. 180 (2007) 859–865.
[28] S. Obbade, C. Dion, M. Rivenet, M. Saadi, F. Abraham, J. Solid State Chem. 177 (2004) 2058–2067.
[29] S. Obbade, C. Renard, F. Abraham, J. Solid State Chem. 182 (3) (2009) 413–420.
[30] P.C. Burns, M.L. Miller, R.C. Ewing, Can. Miner. 34 (1996) 845–880.
[31] P.C. Burns, Can. Miner. 43 (2005) 1839–1894.
[32] V. Petricek, M. Dusek, L. Palatinus, Jana2000. Structure Determination Software Programs, Institute of Physics, Praha, Czech Republic, 2005.
[33] SAINT Version 7.06a, Bruker AXS Inc., Madison, WI, USA, 2004.
[34] SADABS 2004/1, Bruker AXS Inc., Madison, WI, USA, 2004.
[35] A. Altomare, M.C. Burla, M. Camalli, G. Cascarano, C. Giacovazzo, A. Guagliardi, A.G.G. Moliterni, G. Polidori, R. Spagna, SIR97. A Package for Crystal Structure Solution by Direct Methods and Refinement, Bari, Rome, Italy, 1997.
[36] M.E. Bresse, M. O'Keeffe, Acta Crystallogr. B 47 (1991) 192–197.
[37] I.D. Brown, D. Altermatt, Acta Crystallogr. B 41 (1985) 244–247.
[38] P.C. Burns, R.C. Ewing, R.C. Hawthorne, Can. Miner. 35 (1997) 1551–1570.
[39] S.A. Linde, Y.E. Gorbunova, A.V. Lavrov, Z. Neorg. Khim. 25 (1980) 1992–1994.
[40] B.O. Loopstra, Acta Crystallogr. B 26 (1970) 656–657.
[41] J.D. Woodward, T.E. Albrecht-Schmitt, J. Solid State Chem. 178 (2005) 2922–2926.
[42] C. Dion, S. Obbade, E. Raekelboom, F. Abraham, J. Solid State Chem. 155 (2000) 342–353.
[43] F. Demartin, C.M. Gramaccioli, T. Pilati, Acta Crystallogr. B 48 (1992) 1–4.
[44] N.N. Krot, M.S. Grigoriev, Russ. Chem. Rev. 73 (2004) 89–100.
[45] Y.P. Li, C.L. Cahill, P.C. Burns, Chem. Mater. 13 (2001) 4026–4031.
[46] S. Obbade, S. Yagoubi, C. Dion, M. Saadi, F. Abraham, J. Solid State Chem. 177 (2004) 1681–1694.
[47] T.A. Sullens, R.A. Jensen, T.Y. Shvareva, T.E. Albrecht-Schmitt, J. Am. Chem. Soc. 126 (2004) 2676–2677.
[48] V.N. Serezhkin, V.K. Trunov, L.G. Makarevich, Kristallogr 25 (1980) 858–860.
[49] N.P. Brandenburg, B.O. Loopstra, Acta Crystallogr. B 34 (1978) 3734–3736.
[50] J.C. Taylor, P.W. Wilson, Acta Crystallogr. B 29 (1973) 1073–1076.
[51] S.A. Miller, J.C. Taylor, Z. Kristallogr. 177 (1986) 247–253.
[52] M.H. Chisholm, C.C. Lin, J.C. Galluci, B.T. Kob, Dalton Trans. (2003) 406–412.
[53] Y. Tang, L.N. Zakharov, A.L. Rheingold, R.A. Kemp, Polyhedron 24 (13) (2005) 1738–1748.